doi:10.1016/S0022-2836(02)01334-7 *J. Mol. Biol.* (2003) **326**, 167–175

JMB

Available online at www.sciencedirect.com

SCIENCE DIRECT®

Deriving Topological Constraints from Functional Data for the Design of Reagentless Fluorescent Immunosensors

Martial Renard, Laurent Belkadi and Hugues Bedouelle*

Department of Structural Biology and Chemistry (CNRS URA 2185), Institut Pasteur 28 Rue de Docteur Roux 75724 Paris, Cedex 15, France

The possibility of obtaining, from any antibody, a fluorescent conjugate which responds to the binding of the antigen by a variation of fluorescence, would be of great interest in the micro- and nano-analytical sciences. This possibility was explored with antibody mAb4E11, which is directed against the dengue virus and for which no structural data is available. Three rules of design were developed to identify residues of the antibody to which a fluorophore could be chemically coupled, after changing them to cysteine by mutagenesis. (i) The target residue belonged to the hypervariable loops of the antibody. (ii) It was adjacent, along the amino acid sequence of the antibody, to a residue which was functionally important for the interaction with the antigen. (iii) It was not important in itself for the interaction with the antigen. Eight conjugates between a single chain variable fragment of mAb4E11 and an environment-sensitive fluorophore were constructed. Three of them showed an increase in their fluorescence intensity by 1.5–2.8-fold on antigen binding, without loss of affinity. This increase allowed the titration of the antigen in serum above a threshold concentration of 10 nM. Experiments of quenching with potassium iodide suggested that the fluorescence variation was due to a shielding of the fluorescent group from the solvent by the binding of the antigen, and that therefore its mechanism is general.

*Corresponding author

Keywords: antibody; biosensor; dengue virus; fluorescence; protein design

Introduction

A biosensor comprises two major components: a biological receptor, which specifically recognizes a ligand, and a transducer, which detects the recognition event and transforms it into a measurable signal. A biosensor functions reagentless if the different steps going from the ligand recognition to the signal measurement do not imply any change in its composition. This characteristic is necessary for a continuous measurement. Monoclonal antibodies seem ideally suited to provide the biological receptor of biosensors, since they can be directed against most haptens or macromolecules. However, they are not adapted to the simple mechanisms of signal transduction.[1]

Several solutions have been developed to solve this problem of signal transduction by antibodies. Some consist in labelling *in vitro* all the proteins of the sample under analysis, as in the present use of antibody micro-arrays.[2,3] Others measure the mass increase on the binding of the antigen to the immobilized antibody, by means of apparatuses based on surface plasmon resonance or piezoelectric quartz microcrystals.[4,5] However, most of these solutions do not allow either continuous or high throughput measurements.

About 15 years ago, a general solution to the problem of signal transduction by antibodies was suggested. North has proposed the insertion of a reporter group close to the paratope (binding-site) of the antibody, for example a fluorophore that is sensitive to changes in its electronic environment.[6] Schultz and co-workers have proposed to use oligonucleotide-directed mutagenesis to

Abbreviations used: mAb, monoclonal antibody; Fv, variable fragment; scFv, single chain Fv; V_H and V_L, variable domains of the heavy chain and light chain, respectively; L-Asn96, residue Asn96 of V_L; L-N96C, mutation of L-Asn96 into Cys; DE1, envelope protein of the dengue virus (serotype DEN1); K_D, dissociation constant; FU, fluorescence unit; SE, standard error; CDR, complementarity determining region.

E-mail address of the corresponding author: hbedouel@pasteur.fr

introduce a cysteine in a specific site of the antibody paratope, chosen on the basis of the crystal structure, then to chemically couple a reactive fluorophore to this mutant Cys.[7] To be operational, the resulting conjugate must obviously show a variation of fluorescence on antigen binding that is measurable, and have an affinity for the antigen that is comparable to the one of the parental antibody. Recently and for the first time, we demonstrated the feasibility of this general approach.[8] We developed quantitative rules of design, based mainly on the crystal structure of the complex between antibody and antigen, to choose the site of fluorophore coupling. We applied these rules to a single chain variable fragment (scFv) of antibody mAbD1.3, which is directed against hen egg white lysozyme and for which numerous structural and functional data are available. In all, 60% of the tested residues gave operational biosensors. Two observations were instrumental in our demonstration. We found that a mild reducing treatment was necessary to reactivate the mutant cysteine residue before its coupling with a reactive fluorophore, and that the reactions of reduction and coupling could be adjusted so as to preserve the essential disulphide bonds of the antibody variable domains.

To be useful, the above approach must imperatively be generalized to antibodies of unknown structure, because structural data are rarely available. Here, we used the following rationale for this generalization. First, we considered that an antibody residue that contributes to the energy of interaction with an antigen, is generally located in the neighbourhood of the antigen in the corresponding complex. The apparent contribution of a residue to an interaction energy can be measured easily, by mutagenesis. Second, we considered that residues that are adjacent in the sequence of a protein, are necessarily adjacent in its spatial structure. These two considerations imply that an antibody residue that is immediately adjacent, along the sequence, to a residue that is energetically important for the interaction with an antigen, will often be located in the three-dimensional neighbourhood of the antigen in the corresponding complex without contributing to its binding. Such a residue constitutes a target of choice for the coupling of an environment-sensitive fluorophore. Thus, sequence and mutagenesis data might be sufficient to deduce the topological data that are necessary for the design of a fluorescent biosensor.

We used mAb4E11, a murine monoclonal antibody (mAb), which is directed against the dengue virus (serotype DEN1) and whose three-dimensional structure is unknown, to test this new approach. The dengue virus infects 2% of the world population every year, i.e. 100 millions of individuals. It can induce a haemorragic fever or shock and be deadly. It is an expanding re-emerging disease. Up until now, no vaccine or specific treatment is available.[9,10] The epitope of mAb4E11 is included within domain 3 (residues 296–400) of the viral envelope protein Env.[11] A recombinant Fab fragment, derived from mAb4E11, and domain 3 of Env can be produced in *Escherichia coli* and purified in quantity.[12] We showed that mutagenesis data on the CDR3 hypervariable loops of Fab4E11 were sufficient to choose sites of coupling for a fluorophore and obtain operational fluorescent conjugates with a high success rate. We used experiments of quenching with potassium iodide (KI) to explore the physico-chemical mechanism by which the fluorescence of the conjugates varied on antigen binding, and showed that this mechanism is general. Our results pave the way to the fast generation of reagentless fluorescent biosensors from any antibody, for fundamental or applied purposes.

Results

Search for coupling sites

We chose the sites of fluorophore coupling in mAb4E11, according to the following rules of design. (1) The target residue was in the hypervariable loops of the antibody, as defined by Chothia.[13] (2) It was adjacent, along the amino acid sequence of the antibody, to a residue that is functionally important for the interaction with the antigen. (3) It was not important itself for the interaction with the antigen. We considered that this last condition was fulfilled if the change of the target residue into alanine decreased the free energy of interaction $\Delta\Delta G$ between antibody and antigen by less than 1.0 kcal mol^{-1}.

The first two criteria implied that the target residue was in the neighbourhood of the antibody paratope. The third criterium eliminated the residues that were central in the interaction with the antigen, and gave a high probability that the target residue was located in the periphery of the paratope. The only necessary data to choose the coupling sites were thus the sequence of the Fv fragment (V_H and V_L) and functional data on its complementarity determining region (CDR) loops. We have generated such functional data on the CDR3 loops of the Fab fragment from mAb4E11. Each residue of these loops has been changed into alanine by mutagenesis, and the dissociation constant, K_D, between each mutant Fab4E11 fragment and the antigen has been measured by competition ELISA (Table 1). Using the rules above, we identified eight potentially peripheral sites, five in V_L and three in V_H ($\Delta\Delta G = 0$ or $+$ in Table 1).

Construction of conjugates

mAb4E11 was expressed as a single chain variable fragment, scFv4E11. The target residues were changed individually into cysteine by site-directed mutagenesis. The mutant scFv4E11 fragments were expressed in the periplasmic space of *E. coli* and purified by means of their His tag, with yields

Table 1. Use of mutagenesis data on Fab4E11 to choose the sites of fluorophore coupling

Residue	$\Delta\Delta G$	Residue	$\Delta\Delta G$
L-Gln93	+++	H-Gly100	++++
L-Arg94	+	H-Trp101	++++
L-Ser95	++++	H-Glu102	++++
L-Asn96	+	H-Gly103	++++
L-Glu97	0	L-Phe104	0
L-Val98	0	H-Ala105	0
L-Pro99	++++	H-Tyr106	0
L-Trp100	++++		
L-Thr101	0		

Columns 1 and 2, V_L domain; columns 3 and 4, V_H. $\Delta\Delta G$, variation of the free energy of interaction with the antigen at 25 °C on going from the wild-type residue to alanine. In kcal mol^{-1}: 0 = −0.5 to +0.5; + = 0.5 to 1.0; ++ = 1.0 to 1.5; +++ = 1.5 to 2.0; ++++ = >2.0. The sites with $-0.5 < \Delta\Delta G < 1.0$ were chosen for the coupling. $\Delta\Delta G = -RT\ln(K_D(\text{wt})/K_D(\text{mut}))$; wt, wild-type; mut, mutant. The constants of dissociation in solution, K_D, between the Fab4E11 derivatives and MalE-DE1-His_6 were measured by competition ELISA. Data from L.B. *et al.* (unpublished results).

of 380(±80) μg l^{-1} of culture (mean ± SE for different mutants and preparations). However, the scFv4E11(L-N96C) mutant could not be obtained in a soluble state and was not studied further (Table 2). The mutant Cys residue was chemically coupled with the IANBD ester, an environment-sensitive fluorophore. A mild reduction with 2-mercaptoethanol was necessary to reactivate the mutant Cys residue before the coupling reaction.[8] As a result of the reduction and coupling steps, a large proportion (79(±3)%) of the scFv molecules precipitated. However, the remaining soluble molecules were efficiently coupled to the fluorophore (96(±6)% of the molecules). The yields of protein recovery and coupling were very similar for the different mutants of scFv4E11 (Table 2). In the same conditions, a negligible proportion (typically 4%) of the parental scFv4E11(wt) molecules was coupled with IANBD. This coupling was therefore specific for the mutant Cys residue.

Properties of the conjugates

The conjugates were incubated with or without a saturating concentration of the antigen in buffer A, and their intensities of fluorescence F at 535 nm were recorded. The relative variation of fluorescence intensity $\Delta F_\infty/F_0 = (F_\infty - F_0)/F_0$ between the antigen-free and bound states was the highest for the conjugate in position L-Thr101, called scFv(L-T101ANBD), and corresponded to a 2.8-fold increase (Table 2). This increase was accompanied with a blue shift of the maximum emission wavelength by 5.5(±0.5) nm. The variation of the fluorescence signals depended on the specific binding of the antigen since, for several conjugates, it was different when the antigen was derived from the DEN1 or from the DEN2 serotype of the dengue virus (not shown). We considered only the antigen-sensitive conjugates ($|\Delta F_\infty/F_0| \geq 10\%$) in the remainder of this work. The K_Ds between the conjugates and the antigen, measured by competition ELISA, differed by less than two-fold from the value for the parental scFv4E11(wt) fragment ($-0.30 \leq \Delta\Delta G \leq 0.03$ kcal mol^{-1}; Table 2). This result showed that the coupled fluorophore did not interfere with the recognition between the scFv4E11 fragment and its antigen.

The fluorescence intensities of the conjugates at positions L-Glu97, L-Thr101 and H-Ala105 were used to titrate the antigen in buffer A (Figure 1). The titration curves were linear between 10 nM and 100 nM of antigen. The theoretical equation (9), linking the relative variation of fluorescence intensity $\Delta F/F_0 = (F - F_0)/F_0$ to the concentration of antigen, was fitted to the experimental data, with the concentration of functional conjugate, $\Delta F_\infty/F_0$ and K_D as fitting parameters (Materials and Methods). We found that the proportion of functional molecules in the conjugate preparations was equal to 90(±6)%. The values of $\Delta F_\infty/F_0$, determined from the titration assays (Table 3), were identical within errors to those obtained from the endpoint values F_0 and F_∞ (Table 2). The values of K_D, determined from the titration

Table 2. Properties of the fluorescent conjugates at 25 °C

Residue	Coupling yield (%)	Protein yield (%)	K_D (nM)	$\Delta F_\infty/F_0$ (%)
L-Arg94	75	36	0.28 ± 0.03	−8 ± 2
L-Asn96	NA	NA	NA	NA
L-Glu97	90	25	0.37 ± 0.04	74 ± 14
L-Val98	93 ± 19	19 ± 8	0.22 ± 0.02	−10 ± 3
L-Thr101	90 ± 5	21 ± 4	0.36 ± 0.02	182 ± 16
H-Phe104	106	22	NA	0.8 ± 0.1
H-Ala105	82	24	0.21 ± 0.02	45 ± 9
H-Tyr106	101	17	NA	2.8 ± 0.3

Column 1, residue of scFv4E11(wt) to which IANBD was coupled after mutation into Cys. Column 2, number of molecules of IANBD / molecule of scFv after coupling. Column 3, protein yield of the reaction steps going from the purified mutant scFv to the conjugate. Column 4, K_D in solution between the conjugate and the MalE-DE1-His_6 antigen, measured by competition ELISA. The K_D value for the parental scFv4E11(wt) was equal to 0.35(±0.06) nM (mean ± SE from three experiments). Column 5, relative variation $\Delta F_\infty/F_0$ of fluorescence intensity between the antigen-free and bound states of the conjugate in buffer A (mean ± SE from two experiments). NA, non-available.

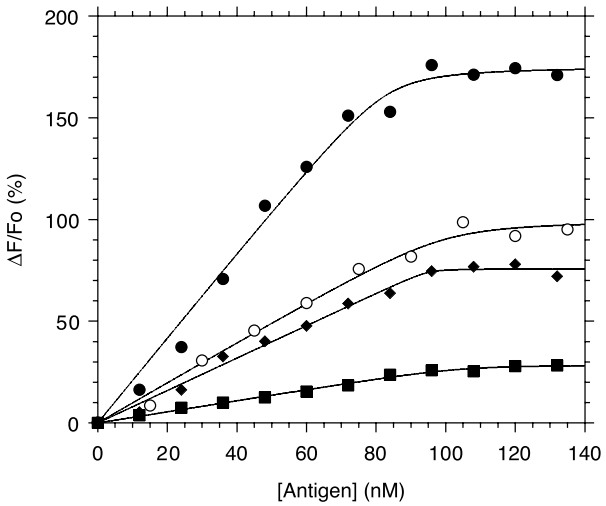

Figure 1. Titration of the MalE-DE1-His_6 antigen by scFv4E11 conjugates at 25 °C, as monitored by fluorescence. The fluorescence intensity of the reaction mixture was measured at 535 nm and the intensity of the free antigen was substracted to obtain the specific intensity F of the scFv conjugate (equation (7)). The graph gives the relative variation of fluorescence intensity $\Delta F/F = (F - F_0)/F_0$ for the conjugate as a function of the total concentration in antigen, where F_0 is the value of F in the absence of antigen. The total concentration of conjugate, measured by $A_{280\ nm}$, was equal to 100 nM. In buffer A: (●) scFv4E11(L-T101ANBD); (◆) scFv4E11-(L-E97ANBD); (■) scFv4E11(H-A105ANBD). In calf serum: (○) scFv4E11(L-T101ANBD). The continuous curves were obtained by fitting equation (9) to the titration data. See Materials and Methods for details.

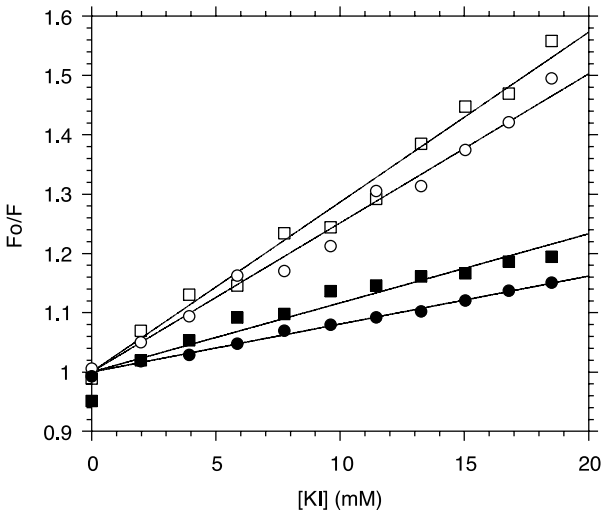

Figure 2. Quenching of the scFv4E11(L-T101ANBD) fluorescence, in its antigen-free or bound state, by KI. F and F_0, fluorescence intensities of the conjugate at 535 nm in buffer A with or without quencher, respectively. (□) and (○) Conjugate in its free state (100 nM) at 25 °C and 15 °C, respectively. (■) and (●) Complex between the conjugate (100 nM) and MalE-DE1-His_6 (300 nM) at 25 °C and 15 °C, respectively. The continuous curves were obtained by fitting the Stern–Volmer equation (10) to the experimental data (Materials and Methods).

assays with high concentrations of total conjugate (100 nM) and antigen (10–150 nM), were consistent with the values obtained by competition ELISA under more satisfying experimental conditions (Tables 2 and 3).

The spectra of the scFv(L-T101ANBD) conjugate were similar in serum and in buffer A, even though the serum had a high intrinsic fluorescence. The titration curves of the antigen by the scFv-(L-T101ANBD) conjugate were also similar in serum and in buffer A (Figure 1). Thus, the properties of this conjugate, i.e. its ability to specifically titrate the antigen in a complex mixture like serum and its high affinity for the antigen, corresponded to the distinctive attributes of a biosensor.[14] The value of $\Delta F_\infty/F_0$ was twofold lower in serum than in buffer A (100(±14)% *versus* 198(±28)%; Table 3). To explain this difference, we compared the molar fluorescences of the free scFv4E11(L-T101ANBD) conjugate and of its complex with the antigen, F_p and F_c, respectively, in serum ($F_p = 0.40(\pm 0.02)$ FU nM^{-1}, $F_c = 0.81(\pm 0.06)$ FU nM^{-1}) and in buffer A ($F_p = 0.56(\pm 0.03)$ FU nM^{-1}, $F_c = 1.7(\pm 0.1)$ FU nM^{-1}). We observed that the fluorescence was quenched in serum relative to buffer A and that the quenching was greater for the bound than for the free scFv4E11 conjugate (2.1 *versus* 1.4-fold). Therefore, the lower variation of fluorescence in serum was due to a differential quenching of the scFv4E11 conjugate, as we previously found and reported for a fluorescent derivative of antibody mAbD1.3.[8] If such a differential quenching is general, a conjugate with 10% $< \Delta F_\infty/F_0 <$ 20% in a defined buffer might be non-operational in serum.

Table 3. Parameters for the titration of conjugates with MalE-DE1-His_6 at 25 °C

Residue	Buffer	Active molecules (nM or %)	K_D (nM)	$\Delta F_\infty/F_0$ (%)
L-Thr101	Tris	80 ± 4	0.88 ± 1.18	198 ± 28
L-Thr101	Serum	96 ± 5	0.34 ± 1.09	100 ± 14
L-Glu97	Tris	94 ± 4	0.29 ± 0.02	78 ± 8
H-Ala105	Tris	104 ± 5	0.68 ± 1.22	28 ± 4

The experimental conditions were the same as for Figure 1. The total concentration of the scFv4E11 conjugate, measured by $A_{280\ nm}$, was equal to 100 nM. Column 1, residue of scFv4E11(wt) to which IANBD was coupled after mutation into Cys. Columns 3–5, values of the concentration in active molecules of conjugate, K_D, $\Delta F_\infty/F_0$, and associated standard errors, obtained by fitting equation (9) to the experimental data. The value of K_D was poorly defined in these experiments because of the high concentrations of conjugate and antigen.

Mechanism of fluorescence variation

We used KI as a probe to explore the physicochemical mechanism by which the fluorescence intensity of the conjugate varied on antigen binding. We first checked by an indirect ELISA

that KI, below 20 mM, did not affect the binding of the parental scFv4E11(wt) fragment to its immobilized antigen. We found that the fluorescence of the scFv4E11(L-T101ANBD) conjugate was quenched by KI (Figure 2). The quenching increased with temperature. This increase indicated that the quenching followed a collisional mechanism.[15] The quenching varied linearly with the concentration of KI. This law of variation indicated that the molecules of fluorophore constituted a homogeneous population and were identically exposed to KI.[15] It confirmed that the fluorescent group was specifically coupled to the mutant cysteine.

The Stern–Volmer constants were higher for the free conjugate than for its complex with the antigen: $K_{SV} = 25.1(\pm 0.5)\ M^{-1}$ *versus* $8.1(\pm 0.1)\ M^{-1}$ at 15 °C; $K_{SV} = 28.6(\pm 0.6)\ M^{-1}$ *versus* $8.7(\pm 0.2)\ M^{-1}$ at 25 °C (SE in the curve fits of Figure 2). These constants depend on the accessibility of the fluorescent group to iodide, the rate constant of collision between the two (k_0), and the fluorescence lifetime of the conjugate in the absence of iodide (τ_0), as described by equation (11). We calculated the values of k_0 for the antigen-free and bound states of the scFv4E11 conjugate, from the Smoluchowski equation (12), the Stokes–Einstein equation (13), the ionic radius of I^-, and the Stokes radii of the conjugate in its different states. These Stokes radii were measured by size exclusion chromatography. We found that the ratio K_{SV}/k_0, and thus the accessibility of the fluorescent group to the I^-, was $3.1(\pm 0.2)$-fold larger in the free conjugate than in the complex with its antigen, both at 15 °C and 25 °C. This variation in the accessibility to the solvent could account for the increase in intensity and blue shift of the conjugate fluorescence on antigen binding.

Discussion

Efficiency of the design rules

Here, we describe new rules of design to choose coupling sites for fluorophores on an antibody and transform it into a reagentless fluorescent biosensor. These rules were based: (1) on the target residue belonging to the neighbourhood of functionally important residues along the sequence of the antibody, and (2) on its absence of functional importance for the interaction with the antigen. We validated these rules with antibody mAb4E11, whose three-dimensional structure is unknown. Among the eight sites satisfying these sequence-based rules of design and belonging to the CDR3 loops of V_H and V_L, four gave operational conjugates ($|\Delta F_\infty/F_0| \geq 10\%$, same affinity as the parental scFv fragment for the antigen). In a previous study on antibody mAbD1.3 and its antigen lysozyme, we have established and validated other rules of design. These rules were based: (1′) on the target residue belonging to a topological neighbourhood of the antigen in the crystal structure of the complex between antibody and antigen, and (2′) on its absence of functional importance for the interaction with the antigen. Among the ten sites of FvD1.3 satisfying these structure-based rules of design, six gave operational conjugates.[8] Thus, our new rules of design, which relied only on sequence and mutagenesis data, were as efficient as our previous rules, which relied heavily upon the knowledge of the crystal structure of the complex between antibody and antigen.

Our results further showed that three-dimensional topological data on the interaction between an antibody and an antigen can be generated from sequence and function data alone and be precise enough to predict an electronic change in the environment of a residue. A structural model of the Fv4E11 fragment, modelled from the amino acid sequences of its V_L and V_H domains by homology (Materials and Methods), confirmed that the residues that gave operational conjugates, were spatially located in the periphery of functionally important residues, not only along the uni-dimensional sequence but also in the three-dimensional spatial structure (Figure 3). In summary, the three-dimensional structure of the complex between antibody and antigen is unnecessary to obtain operational conjugates with a high success rate.

Properties of the operational residues

The residues that gave operational conjugates for antibodies mAb4E11 and mAbD1.3, had the following properties in common. They were mostly hydrophilic (2/4 for mAb4E11; 7/7 for mAbD1.3), preferentially located in the V_L domain (3/4 for mAb4E11; 6/7 for mAbD1.3), and either Tyr residues or in the immediate proximity of Trp, Tyr or Phe residues along the sequence (this work and Ref. 8). These properties of the operational residues probably reflected their exposure to the solvent in the structure of the free antibody, the stronger involvement of the V_H residues, relative to V_L, in the binding of antigens and the general importance of aromatic residues in the interactions between proteins, respectively.[16–18] The application of these three criteria alone would have led to the correct choice of residue L-Thr101 for mAb4E11 and of all the residues that gave operational conjugates for mAbD1.3. Thus, as more operational conjugates are obtained, the basic design rules that we propose here, could be refined and their efficiency improved. Ultimately, the change of a few residues, chosen only from sequence analysis, into Cys by mutagenesis may be sufficient to obtain an operational fluorescent immunosensor from any antibody.

Generalization to other systems

The variation in the fluorescence of the scFv4E11(L-T101ANBD) conjugate on antigen

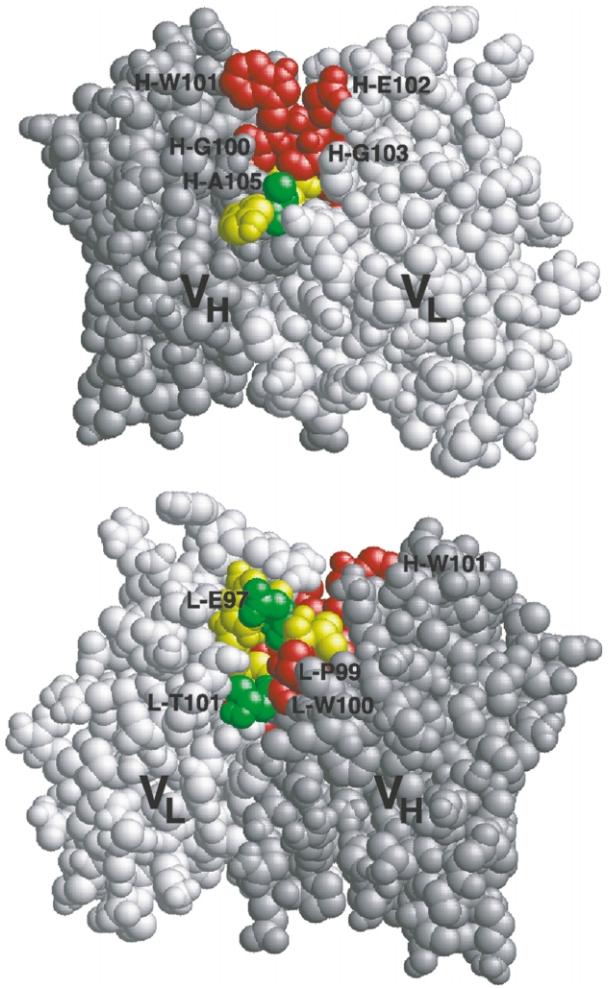

Figure 3. Position of the coupling sites in a model structure of the free Fv4E11 fragment: light grey, V_L; medium grey, V_H; green, coupling sites which gave antigen-sensitive conjugates; red, functionally important residues for the interaction with the antigen; yellow (unlabelled), other residues of the CDR3 loops of V_L and V_H.

binding was due to the shielding of the fluorescent group from the solvent and not to an idiosynchratic property of either the antibody or the antigen. This mechanism suggests that the type of fluorescent conjugate that we describe here, could be extended to other couples of either antigen and antibody, or receptor and ligand. Could this extension be made to antibodies directed against haptens? It might be difficult to find a coupling site that gives an operational conjugate against a hapten antigen through the same physico-chemical mechanism as against a polypeptide antigen: first, because the paratope of the antibody, and thus its neighbourhood, will comprise a lower number of residues; and second, because the shielding of the fluorophore from the solvent upon complex formation will be more limited. However, several studies have shown that the coupling of a fluorophore in the neighbourhood of an enzyme or receptor active site can allow one to monitor the binding of low molecular weight ligands.[7,19,20] In such cases, the change of fluorescence likely results from mechanisms other than the one described above, e.g. a direct quenching or immobilization of the fluorophore by the ligand, or the re-orientation of the fluorophore by the ligand towards a region of the receptor with different physico-chemical properties.

Potential applications

Antibody chips, on which monoclonal or recombinant antibodies are arrayed, have been described.[3,21] They enable the passive capture of ligands but are unable to transduce the event of capture into a measurable signal. Thus, they necessitate the coupling of a dye to the preparation of analysed proteins, generally the whole proteome of either a cell, a cellular compartment, or a body fluid. Such a coupling meets with the following difficulties. The coupling of dyes to proteins strongly depends on the physico-chemical properties of the reaction buffer for its efficiency, and therefore may be poorly reproducible in the case of cellular extracts.[22] The reaction of dye coupling introduces a delay before the measurement, during which the proteome may evolve, for example by degradation. The non-specific coupling of a dye with a protein may interfere with its recognition by antibodies. Finally, some proteins may not possess chemical groups that are reactive for the coupling of a dye.

Antibody chips could be transformed into immunosensor chips by using the approach that we described here. The use of immunosensor chips would eliminate the need for coupling a dye to the whole preparation of proteins under analysis. They would enable one to measure directly the concentration of antigens. Immunosensor chips, associated with a microfluidic system, could enable one to detect and measure the concentration of a large number of antigens simultaneously in a few microlitres of sample. It remains to be determined if the sensitivity of antigen detection by a fluorescent immunosensor could equal that which is attained by the labelling of the antigen, and if the conjugates that we constructed in this study, could be used for the diagnosis of dengue virus infections.

Recently, the construction of biosensors on a nanometric scale has constituted a major breakthrough in the field of analytical sciences. The tip of an optical nanofibre was coated with an antibody and introduced into a single living cell to measure the concentration of an intrinsically fluorescent hapten.[23] The replacement of the antibody by a reagentless fluorescent immunosensor would allow the continuous measurement of any non-fluorescent antigen, intracellularly. The immobilization of fluorescent immunosensors at the tip of optical fibres could also allow one to continuously measure the concentration of specific

neurotransmitters within the brain, and thus provide a gateway to new fields of research in the neuro and behavioral sciences.

In conclusion, we have described and validated a new, fast and general approach, which is knowledge-based and relies only on sequence and mutagenesis data, to generate reagentless fluorescent biosensors from any monoclonal antibody. Such antibodies can be obtained by the hybridoma technology or from combinatorial libraries.[24–30] Reagentless fluorescent immunosensors should provide new analytical tools for fundamental research and have many applications in the fields of health, environment, civil defence and industrial processes.

Materials and Methods

Recombinant plasmids and proteins

Plasmid pLB1, coding for the scFv of mAb4E11, had the same structure as pMR1, coding for scFvD1.3,[8] except that the sequences coding for V_H and V_L were specific for mAb4E11. They were retrieved from plasmid pMad4E11, coding for Fab4E11, by PCR[12] (L.B. *et al.*,unpublished results). scFv4E11 carried the same His_6 extension at its C-terminal end as scFvD1.3. Selected residues of scFv4E11 were changed into cysteine by oligonucleotide site-directed mutagenesis as described.[8] The antigen of mAb4E11 was produced in the periplasm of *E. coli* and purified to homogeneity as a hybrid, MalE-DE1(296–400)-His_6 (noted as MalE-DE1-His_6), between the *E. coli* MalE protein, residues 296–400 of the dengue virus envelope protein (serotype DEN1), and a His_6 tag[12] (L.B. *et al.*,unpublished results).

Production, purification and coupling

The production of the scFv4E11 derivatives, their purification by means of their His_6 tag, and the coupling of the IANBD ester (*N*-((2-(iodoacetoxy)ethyl)-*N*-methyl)-amino-7-nitrobenz-2-oxa-1,3-diazole, Molecular Probes) to the mutant cysteine residues were performed as described[8] with two exceptions: the reduction by 10 mM 2-mercaptoethanol was for 30 minutes at 37 °C for scFv(L-V98C) and at 30 °C for all the other mutants; and the coupling of the fluorophore was for two hours at 30 °C with agitation. The concentrations of MalE-DE1-His_6, of the scFv4E11 mutants and of their conjugates with IANBD, and the coupling yields were measured by absorbance spectrometry, with $\varepsilon_{280\ nm}$(MalE-DE1-His_6) = 76.445 $mM^{-1}\,cm^{-1}$, $\varepsilon_{280\ nm}$(scFv4E11) = 48.15 $mM^{-1}\,cm^{-1}$,[31] $\varepsilon_{280\ nm}$(ANBD) = 2.1 $mM^{-1}\,cm^{-1}$ and $\varepsilon_{500\ nm}$(ANBD) = 31.8 $mM^{-1}\,cm^{-1}$.[8]

Competition ELISA

The dissociation constants K_D were measured by competition ELISA.[32,33] The scFv fragment (10^{-10} M) and the MalE-DE1-His_6 antigen were mixed in solution (PBS buffer, 1% (w/v) BSA), and the binding reaction was left to equilibrate overnight. The concentration of free scFv in the reaction mixture was measured by an indirect ELISA, in which MalE-DE1 (without His_6 tag) was immobilized and the captured scFv was revealed through its His_6 tag, with an anti-His_5 antibody (Qiagen).

Titration experiments

The scFv4E11 conjugates (100 nM) were titrated with increasing concentrations of MalE-DE1-His_6. The conjugate and antigen were mixed and left for one hour at 25 °C in the dark to equilibrate. They form a complex according to the reaction:

$$P + L \leftrightarrow P : L \tag{1}$$

where P is the conjugate; L, its antigen; and P:L, their complex. The law of mass conservation gives:

$$[P]_0 = [P] + [P : L] \text{ and } [L]_0 = [L] + [P : L] \tag{2}$$

where [L], [P] and [P:L] are concentrations; and $[P]_0$ and $[L]_0$ are the total concentrations of P and L in the reaction, respectively. At equilibrium, the law of mass action gives:

$$K_D = [P][L]/[P : L] \tag{3}$$

where K_D is the dissociation constant between P and L. Combining equations (2) and (3) gives:

$$[P : L]^2 - [P : L](K_D + [P]_0 + [L]_0) + [P]_0[L]_0 = 0 \tag{4}$$

whose solution is given by:

$$[P : L] = \frac{\{K_D + [P]_0 + [L]_0 - ((K_D + [P]_0 + [L]_0)^2 - 4[P]_0[L]_0)^{1/2}\}}{2} \tag{5}$$

Fluorescence measurements

The protein and serum preparations were centrifuged before use, to remove any aggregate. The fluorescence measurements were performed with a LS-5B spectrofluorometer (Perkin–Elmer) either in buffer A (150 mM NaCl, 50 mM Tris–HCl, pH 7.5) or in calf serum. The fluorescence was excited at 480 nm (5 nm slit width) and measured at 535 nm (20 nm slit width). The global intensity of fluorescence F', measured for the reaction mixture between the antigen L and the conjugate P, was decomposed according to the following equation:

$$F' = F_l[L] + F_p[P] + F_c[P : L] + F_b \tag{6}$$

where F_l, F_p and F_c were the molar intensities of fluorescence for L, P, and their complex P:L, respectively; and F_b, the signal of the buffer alone. Combining equations (2) and (6) gave:

$$F = F' - (F_b + F_l[L]_0) = F_p[P]_0 + (F_c - F_l - F_p)[P : L] \tag{7}$$

The signal of L alone was measured in an independent experiment and substracted from the global signal F' of the reaction mixture to give the specific signal F of the conjugate. The signal of L alone was also used to determine the value of F_l, which was found to be less than $0.01F_p$ and therefore neglected. According to equation (7), the values F_0 and F_∞ of F at zero and saturating concentrations of L are given by:

$$F_0 = F_p[P]_0 \text{ and } F_\infty = (F_c - F_l)[P]_0 \tag{8}$$

Equation (7) was therefore rearranged as follows:

$$(F - F_0)/F_0 = \Delta F/F_0 = (\Delta F_\infty/F_0)([P : L]/[P]_0) \tag{9}$$

The values of $\Delta F_\infty/F_0$, $[P]_0$ and K_D could be determined by fitting equation (9), in which [P:L] is given by equation (5), to the experimental values of $\Delta F/F_0$, measured in titration experiments.

Quenching by iodide

The experiments were performed in buffer A, as described above. The Stern–Volmer equation (10) was fitted to the experimental data, where F and F_0 are the intensities of fluorescence for the scFv conjugate, with or without quencher, respectively. F_0 and the Stern–Volmer constant K_{SV} were used as fitting parameters:

$$F^{-1} = (1 + K_{SV}[KI])F_0^{-1} \quad (10)$$

K_{SV} was decomposed according to equation (11), where τ_0 is the lifetime of the fluorophore excited-state in the absence of quencher; f_q, the proportion of collisions leading to an extinction of the fluorophore; and k_0, the bimolecular rate constant of collision:[15]

$$K_{SV} = \tau_0 f_q k_0 \quad (11)$$

k_0 was calculated with the Smoluchowski equation (12), where N is the Avogadro number; D_f and D_q, the diffusion coefficients of the conjugate and iodide, respectively; and R_f and R_q, the Stokes and ionic radii of the conjugate and iodide, respectively:

$$k_0 = 4000\pi N(D_f + D_q)(R_f + R_q) \quad (12)$$

The diffusion coefficents were calculated with the Stokes–Einstein equation (13), where k is the Boltzman constant; T, the absolute temperature; η, the viscosity of water at T; and R, either R_f or R_q:

$$D = kT(6\pi\eta R)^{-1} \quad (13)$$

The numerical values of the parameters were the following: $\eta = 0.902 \times 10^{-3}$ kg m^{-3} at 25 °C and 1.161×10^{-3} kg m^{-3} at 15 °C for water; $R_q = 2.06 \times 10^{-10}$ m for the I^-;[34] $R_f = 2.33 \times 10^{-9}$ m for the free conjugate; $R_f = 3.52 \times 10^{-9}$ m for the complex between conjugate and antigen. The values of R_f were determined as described below.

Determination of the Stokes radii

The Stokes radius of the scFv4E11(L-T101ANBD) conjugate was considered as identical with that of the parental scFv4E11(wt). The Stokes radii of scFv4E11(wt), either free or in complex with MalE-DE1-His$_6$, were measured by size exclusion chromatography on a Superdex 75 HR 10/30 column (Amersham Biosciences), in buffer A at room temperature, essentially as described.[35]

Structural modelling

The three-dimensional structure of the Fv4E11 fragment was modeled with the WAM program.[36] The N-terminal residue of the V_H domain, which had been added during the cloning procedure, was ignored.[12] The correctess of the modelled structure was verified with the PROCHECK program.[37]

Acknowledgements

We thank Shamila Naïr for critical reading of the manuscript and Philippe Thullier for the gift of plasmid pMad4E11. This research was funded by grants from the French Ministry of Defense to H.B. (DGA No. 20216/DSP/SREA/F) and from the Fondation pour la Recherche Médicale to M.R. (FRM No. FDT20020920140/1).

References

1. Morgan, C. L., Newman, D. J. & Price, C. P. (1996). Immunosensors: technology and opportunities in laboratory medicine. *Clin. Chem.* **42**, 193–209.
2. MacBeath, G. & Schreiber, S. L. (2000). Printing proteins as microarrays for high-throughput function determination. *Science*, **289**, 1760–1763.
3. Haab, B. B., Dunham, M. J. & Brown, P. O. (2001). Protein microarrays for highly parallel detection and quantitation of specific proteins and antibodies in complex solutions. *Genome Biol.* **2** research0004.1–0004.13.
4. Karlsson, R., Michaelsson, A. & Mattsson, L. (1991). Kinetic analysis of monoclonal antibody-antigen interactions with a new biosensor based analytical system. *J. Immunol. Methods*, **145**, 229–240.
5. Muratsugu, M., Ohta, F., Miya, Y., Hosokawa, T., Kurosawa, S., Kamo, N. & Ikeda, H. (1993). Quartz crystal microbalance for the detection of microgram quantities of human serum albumin: relationship between the frequency change and the mass of protein adsorbed. *Anal. Chem.* **65**, 2933–2937.
6. North, J. R. (1985). Immunosensors: antibody-based biosensors. *Trends Biotechnol.* **3**, 180–186.
7. Pollack, S. J., Nakayama, G. R. & Schultz, P. G. (1988). Introduction of nucleophiles and spectroscopic probes into antibody combining sites. *Science*, **242**, 1038–1040.
8. Renard, M., Belkadi, L., Hugo, N., England, P., Altschuh, D. & Bedouelle, H. (2002). Knowledge-based design of reagentless fluorescent biosensors from recombinant antibodies. *J. Mol. Biol.* **318**, 429–442.
9. Rigau-Perez, J. G., Clark, G. G., Gubler, D. J., Reiter, P., Sanders, E. J. & Vorndam, A. V. (1998). Dengue and dengue haemorrhagic fever. *Lancet*, **352**, 971–977.
10. Gubler, D. J. (2002). Epidemic dengue/dengue hemorrhagic fever as a public health, social and economic problem in the 21st century. *Trends Microbiol.* **10**, 100–103.
11. Thullier, P., Demangel, C., Bedouelle, H., Megret, F., Jouan, A., Deubel, V. *et al.* (2001). Mapping of a dengue virus neutralizing epitope critical for the infectivity of all serotypes: insight into the neutralization mechanism. *J. Gen. Virol.* **82**, 1885–1892.
12. Thullier, P., Lafaye, P., Megret, F., Deubel, V., Jouan, A. & Mazie, J. C. (1999). A recombinant Fab neutralizes dengue virus *in vitro*. *J. Biotechnol.* **69**, 183–190.
13. Al-Lazikani, B., Lesk, A. M. & Chothia, C. (1997). Standard conformations for the canonical structures of immunoglobulins. *J. Mol. Biol.* **273**, 927–948.
14. Griffiths, D. & Hall, G. (1993). Biosensors: what real progress is being made? *Trends Biotechnol.* **11**, 122–130.
15. Lakowicz, J. R. (1999). *Principles of Fluorescent Spectroscopy*, 2nd edit., Kluwer Academic/Plenum, New York pp. 237–265.
16. Wilson, I. A. & Stanfield, R. L. (1994). Antibody-antigen interactions: new structures and new conformational changes. *Curr. Opin. Struct. Biol.* **4**, 857–867.
17. Xu, J. L. & Davis, M. M. (2000). Diversity in the CDR3 region of V(H) is sufficient for most antibody specificities. *Immunity*, **13**, 37–45.

18. Bogan, A. A. & Thorn, K. S. (1998). Anatomy of hot spots in protein interfaces. *J. Mol. Biol.* **280**, 1–9.
19. Post, P. L., Trybus, K. M. & Taylor, D. L. (1994). A genetically engineered, protein-based optical biosensor of myosin II regulatory light chain phosphorylation. *J. Biol. Chem.* **269**, 12880–12887.
20. Gilardi, G., Mei, G., Rosato, N., Agro, A. F. & Cass, A. E. (1997). Spectroscopic properties of an engineered maltose binding protein. *Protein Eng.* **10**, 479–486.
21. de Wildt, R. M., Mundy, C. R., Gorick, B. D. & Tomlinson, I. M. (2000). By-passing selection: direct screening for antibody–antigen interactions using protein arrays. *Nature Biotechnol.* **18**, 989–994.
22. Houk, T. W., Ovnic, M. & Karipides, S. (1983). pH and polymerization dependence of the site of labeling of actin by 7-chloro-4-nitrobenzo-2-oxa-1,3-diazole. *J. Biol. Chem.* **258**, 5419–5423.
23. Vo-Dinh, T., Alarie, J. P., Cullum, B. M. & Griffin, G. D. (2000). Antibody-based nanoprobe for measurement of a fluorescent analyte in a single cell. *Nature Biotechnol.* **18**, 764–767.
24. Burton, D. R. & Barbas, C. F., III (1994). Human antibodies from combinatorial libraries. *Advan. Immunol.* **57**, 191–280.
25. Winter, G., Griffiths, A. D., Hawkins, R. E. & Hoogenboom, H. R. (1994). Making antibodies by phage display technology. *Annu. Rev. Immunol.* **12**, 433–455.
26. Vaughan, T. J., Williams, A. J., Pritchard, K., Osbourn, J. K., Pope, A. R., Earnshaw, J. C. *et al.* (1996). Human antibodies with sub-nanomolar affinities isolated from a large non-immunized phage display library. *Nature Biotechnol.* **14**, 309–314.
27. Pini, A., Viti, F., Santucci, A., Carnemolla, B., Zardi, L., Neri, P. & Neri, D. (1998). Design and use of a phage display library. Human antibodies with subnanomolar affinity against a marker of angiogenesis eluted from a two-dimensional gel. *J. Biol. Chem.* **273**, 21769–21776.
28. de Haard, H. J., van Neer, N., Reurs, A., Hufton, S. E., Roovers, R. C., Henderikx, P. *et al.* (1999). A large non-immunized human Fab fragment phage library that permits rapid isolation and kinetic analysis of high affinity antibodies. *J. Biol. Chem.* **274**, 18218–18230.
29. Knappik, A., Ge, L., Honegger, A., Pack, P., Fischer, M., Wellnhofer, G. *et al.* (2000). Fully synthetic human combinatorial antibody libraries (HuCAL) based on modular consensus frameworks and CDRs randomized with trinucleotides. *J. Mol. Biol.* **296**, 57–86.
30. Hanes, J., Schaffitzel, C., Knappik, A. & Pluckthun, A. (2000). Picomolar affinity antibodies from a fully synthetic naive library selected and evolved by ribosome display. *Nature Biotechnol.* **18**, 1287–1292.
31. Pace, C. N., Vajdos, F., Fee, L., Grimsley, G. & Gray, T. (1995). How to measure and predict the molar absorption coefficient of a protein. *Protein Sci.* **4**, 2411–2423.
32. Friguet, B., Chaffotte, A. F., Djavadi-Ohaniance, L. & Goldberg, M. E. (1985). Measurements of the true affinity constant in solution of antigen-antibody complexes by enzyme-linked immunosorbent assay. *J. Immunol. Methods*, **77**, 305–319.
33. Rondard, P., Goldberg, M. E. & Bedouelle, H. (1997). Mutational analysis of an antigenic peptide shows recognition in a loop conformation. *Biochemistry,* **36**, 8962–8968.
34. Lide, D. R. & Kehiaian, H. V. (1994). *CRC Handbook of Thermophysical and Thermochemical Data*, CRC Press, Boca Raton, Florida USA.
35. Park, Y. C. & Bedouelle, H. (1998). Dimeric tyrosyl-tRNA synthetase from *Bacillus stearothermophilus* unfolds through a monomeric intermediate. A quantitative analysis under equilibrium conditions. *J. Biol. Chem.* **273**, 18052–18059.
36. Whitelegg, N. R. & Rees, A. R. (2000). WAM: an improved algorithm for modelling antibodies on the WEB. *Protein Eng.* **13**, 819–824.
37. Laskowski, R. A., MacArthur, M. W., Moss, D. S. & Thornton, J. M. (1993). Procheck: a program to check the stereochemical quality of protein structure. *J. Appl. Crystallog.* **26**, 283–291.

Edited by J. Karn

(Received 13 August 2002; received in revised form 8 November 2002; accepted 19 November 2002)